Supporting Information

Amide-triazole isosteric substitution for tuning self-assembly and incorporating new functions into soft supramolecular materials

Jürgen Bachl,[a] Judith Mayr,[a] Fracisco J. Sayago,[b] Carlos Cativiela[b] and David Díaz Díaz[ac]*

[a] Universität Regensburg, Fakultät für Chemie und Pharmazie, Institut für Organische Chemie, Universitätsstr. 31, 93053 Regensburg, Germany
[b] Instituto de Síntesis Química y Catálisis Homogénea (ISQCH), CSIC-Universidad de Zaragoza, 50009 Zaragoza, Spain
[c] IQAC-CSIC, Jordi Girona 18-26, Barcelona 08034, Spain

E-mail: David.Diaz@chemie.uni-regensburg.de

Contents List

1. Expanded literature

Besides the application of triazoles in petidomimetics and bioconjugation,[1] they have been also recognized as very useful structural motifs for the fabrication of functional materials in material science.[2] Triazole linker has been employed, for example, for the preparation of sensors,[3] zeolites for gas uptake and catalysis,[4] and gel materials (both chemically and physically crosslinked gels).[5] In addition, triazoles constitute important building blocks for the development of novel drug-systems or for the fabrication of peptidomimetics with broad applications in medicinal chemistry. On the other hand, supramolecular gels and in specific hydrogels have been recognized as promising materials in numerous fields including catalysis, sensing, cosmetics, environmental remediation and biomedicine.[6,7] The physical properties of hydrogels, resembling those of natural systems,[8] combined with the concept of amide-triazole isosteric replacement (Figure S1) could result in the formation of novel materials with interest in bioscience and biotechnology. Many gel-systems have already proven to be suitable systems in controlled and/or sustained drug release.

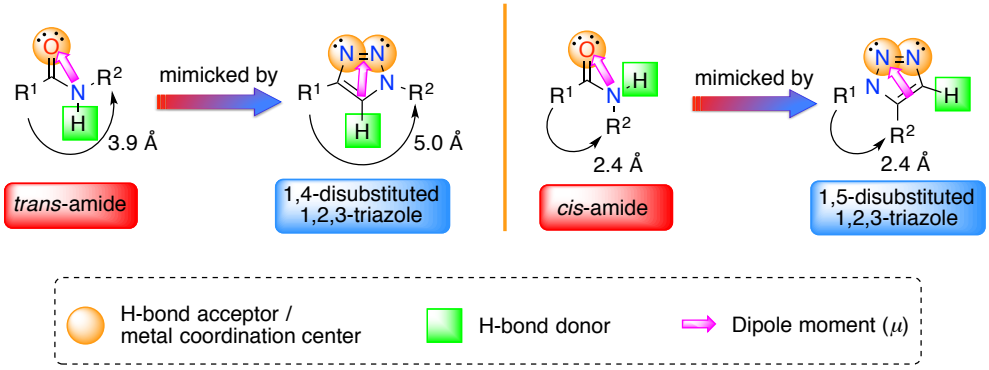

Fig. S1 Summary of the main characteristics of triazole and amide moieties according to their potential bioisosterism. 1,5-Disubstituted triazoles are accessible by the cycloaddition reaction between azides and alkynes catalyzed by $Cp^*RuCl(PPh_3)_2$.[9]

2. General remarks on characterization methods

2.1. Characterization of compounds

a) Thin layer chromatography (TLC) analyses were performed using fluorescent-indicating plates (aluminum sheets precoated with silica gel 60 F_{254}, thickness 0.2 mm, Merck), and visualization achieved by UV light (λ_{max} = 254 nm) and staining with phosphomolybdic acid and/or iodine.

b) Nuclear magnetic resonance (NMR) spectra were recorded at 25 ºC on Bruker Avance-300 instrument. Chemical shifts are denoted in δ (ppm) relative to residual solvent peaks. Coupling constants, *J*, are given in Hertz. The following standard abbreviations are used for characterization of ^{1}H-NMR signals: s = singlet, d = doublet, t = triplet, m = multiplet, dd = doublet of doublets, dt = doublet of triplets. Estimated error of reported values: 0.01 ppm (δ, ^{1}H-NMR), 0.1 ppm (δ, ^{13}C-NMR), 0.1 Hz (*J*, coupling constant).

c) Low-resolution mass spectroscopy was carried out on a Varian MAT 311A.

d) Elemental analyses were performed on a Heraeus Mikro-Rapid analyzer.

e) UV-vis spectroscopy was performed using a Varian Cary 50 UV spectrophotometer and quartz-glass cuvettes of 0.5 cm thickness.

2.2. Characterization of gel-based materials

NOTE: Unless otherwise specified, all reagents, starting materials and solvents (p.a. grade) were purchased from commercial suppliers and used as received without further purification. Double-distilled water was purified additionally using a Millipore water-purifying system (Merck) prior usage. Xylene as mixture of isomers was used after double-distillation.

a) Critical gelation concentration (CGC) values (defined as the minimum concentrations of compound where gelation is observed) were estimated by continuously adding aliquots of solvent (0.02–0.1 mL) into vials containing the potential gelator and performing a typical heating-cooling protocol for gel-formation until no gelation was observed. The starting point for CGC determinations was 200 g L^{-1}.

b) Thermal *gel*-to-*sol* transition temperature (T_{gel}) values were determined using a custom made set-up where the sealed vial was placed into a mold of an alumina block and heated up at 1 °C/5 min using an electric heating plate equipped with a temperature control couple (Figure S2). So obtained values were verified by DSC measurements as well as the inverse flow method (IFM)[10] in which the sealed vial containing the gel material was hung horizontally into an oil bath and heated up at 1 ºC/5 min. It is worth mentioning that the values determined by IFM strongly depend on factors such as cooling rate, aging time, thermal history, and degree of hysteresis [21] among others.

   Herein, the temperature at which the gel started to break was defined as T_{gel}. Each measurement was made at least by duplicate and the average value reported. T_{gel} values were found almost unaltered within a difference of 1–2 ºC after several heating-cooling cycles. Moreover, verification of the independence of the position inside the custom made apparatus was carried out.

c) Fourier transform infrared (FT-IR) spectra were recorded at RT using an Excalibur FTS 3000 FT-IR spectrometer (Biorad) equipped with a single reflection ATR (attenuated total reflection) accessory (Golden Gate, Diamond).

d) Differential scanning calorimetry (DSC) measurements were performed on a Mettler Toledo Differential Scanning Calorimeter using a DSC 30 measuring cell. The DSC thermograms were obtained under dynamic argon atmosphere (gas flow rate = 25 mL min^{-1}) at a heating rate of 10 ºC min^{-1}. Samples were placed in closed aluminum pans (Mettler Toledo). An empty sample holder was used as reference and the runs were performed by heating the samples from 25 to 90 ºC. The values were reported as the average of two independent measurements.

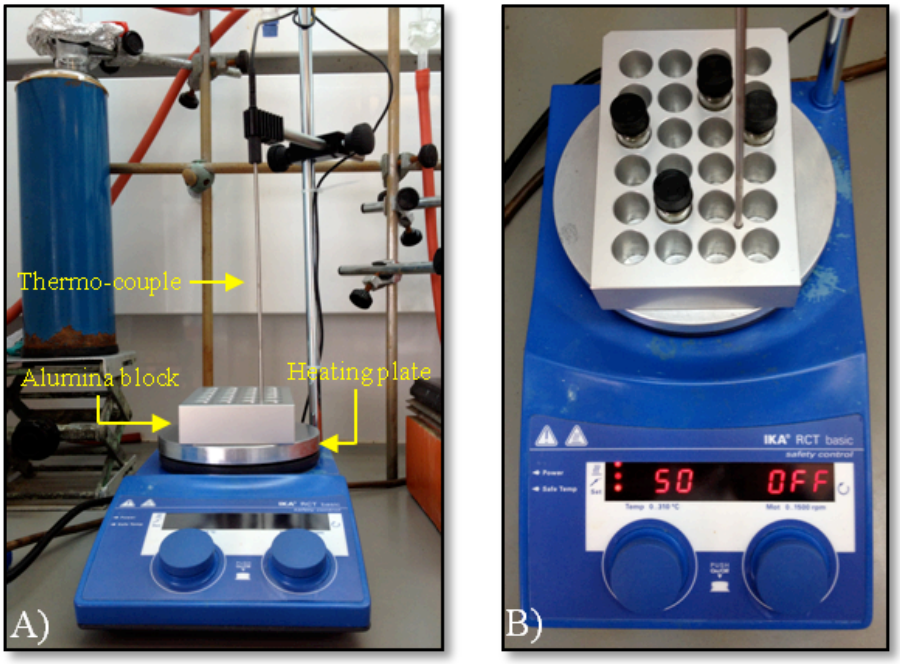

Fig. S2 Custom made set-up for T_{gel} determinations. A) Front view showing the composition between electric heating plate, alumina block and digital thermo-couple. B) Top view of the set-up during experimentation containing vials (4 cm length × 1 cm diameter) with gel materials. It is important to mention that the alumina block was constructed especially for one type of vials, which fit smoothly inside the molds to ensure a good transmission of the heat-flow.

e) Field Emission Scanning Electron Microscopy (FESEM) images of xerogels were obtained with a Zeiss Merlin, Field Emission Scanning Electron Microscope operated at an accelerating voltage of 10 kV. Scanning Electron Microscope (SEM) was performed using a JEOL JSM 6400 scanning electron microscope equipped with a digital camera and operating at 15 kV. For visualization, samples were prepared by the freeze-drying (FD) method. In brief, an Eppendorf tube containing the corresponding gel-material (100–200 μL) was frozen in liquid nitrogen or dry ice/acetone and the solvent immediately evaporated under reduced pressure (0.6 mmHg) for 2 days at RT. The so obtained fibrous solid was placed on top of a tin plate and shielded by Pt (40 mA during 30–60 s; film thickness = 5–10 nm).

f) Oscillatory rheology was performed with an AR 2000 Advanced rheometer (TA Instruments) equipped with a Julabo C cooling system. A 1000 μm gap setting and a torque setting of 40,000 dynes/cm^2 at 25 ºC were used for the measurements in a plain-plate (20 mm, stainless steel). The data were found to be highly reproducible for independent batches. The following experiments were carried out for each sample, using 2 mL total gel volume: a) Dynamic strain sweep (DSS): variation of G' and G'' with strain (from 0.01 to 100%); b) dynamic frequency sweep (DFS): variation of G' and G'' with frequency (from 0.1 to 10 Hz at 0.1% strain); c) dynamic time sweep (DTS): variation of G' and G'' with time keeping the strain and frequency values constant and within the linear viscoelastic regime as determined by DSS and DFS measurements (strain = 0.1% strain; frequency = 1 Hz). Mechanical inertial effects of the measuring head was accounted by the software package to accurate evaluate the thixotropic nature of the materials through loop tests. For this, fixed rest time after sample loading and pre-shearing to equilibrium at different shear rates were routinely made in order to minimize prehistory effects.

g) General procedure for drug release studies: A weighted amount of the corresponding gelator (60 mg = minimum amount necessary to obtain stable gels by coassembly both gelators), and 1 mL of an

aqueous vancomycin stock solution (2 g L^{-1}) were placed in a screw-capped glass vial and gently heated until all solid materials were completely dissolved. The obtained isotropic solution was allowed to cool down to RT resulting in gel formation with physically incorporated vancomycin. Obtained gel materials were overlaid with phosphate buffered saline (PBS, 1 mL, pH = 7.4) 16 h after their formation, which was considered as the starting point for the experiments. At selected points of time aliquots (100 μL) were removed and diluted with PBS to 1 mL. Then fresh PBS (100 μL) was added over the gel to maintain infinite sink conditions. Drug concentration in the aliquots was determined during the experiments using UV-spectroscopy after proper calibration using the maximum absorbance of vancomycin in aqueous media at 280 nm. Samples were centrifuged (EBA 12 Hettich Zentrifugen) at 4000 rpm for 5 min before measurements. It was verified that degraded gel materials exhibited a minimum absorbance in the region of drug detection.

Experiments with different gelator concentrations and compositions and/or with other drugs were carried out in a similar manner.

3. Preparation of isosteric gelators

3.1. Synthesis and characterization of C_{18}-Glu

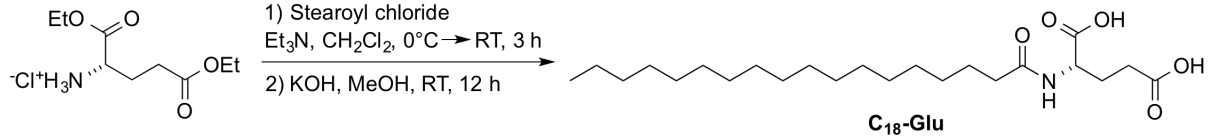

Scheme 1. Synthetic scheme for the preparation of **C_{18}-Glu**.

*(S)-2-Stearamidopentanedioic acid (**C_{18}-Glu**)*

C_{18}-Glu was prepared following the general procedure previously described[11] with slight modifications: To a stirred solution of L-glutamic acid diethyl ester hydrochloride (1.72 g, 7.2 mmol) and NEt_3 (2.17 g, 3.0 mL, 21.5 mmol) in dry methylene chloride (150 mL) at 0 °C, a solution of stearoyl chloride (2.39 g, 7.9 mmol) in dry methylene chloride (20 mL) was added slowly over a period of 1h. The mixture was allowed to warm to RT and stirred for additional 3 h, after which time water (50 mL) was added. The organic layer was separated, washed with water (3 × 50 mL), dried over Na_2SO_4, filtered and the solvent was removed under reduced pressure. The obtained residue was dissolved in a 1:1 mixture of MeOH/water (150 mL) and KOH (1.21 g, 21.5 mmol) was added. The obtained suspension was stirred for 12 h at RT. MeOH was removed under reduced pressure and the aqueous phase was acidified with 2M HCl to pH = 2. The formed precipitate was filtered off, thoroughly washed with water, dried and recrystallized from acetone affording the title compound as white solid in 81% yield (2.40 g, 5.8 mmol). ^{1}H NMR (400 MHz, DMSO-d_6) δ (ppm) = 7.95 (d, J = 7.8 Hz, 1H), 4.19–4.14 (m, 1H), 2.24 (t, J = 7.6 Hz, 2H), 2.08 (td, J = 7.1, 1.5 Hz, 2H), 1.89 (td, J = 13.4, 7.5 Hz, 1H), 1.81–1.67 (m, 1H), 1.48–1.41 (m, 2H), 1.23 (s, 28H), 0.85 (t, J = 6.8 Hz, 3H); ^{13}C NMR (101 MHz, DMSO-d_6) δ (ppm) = 173.73, 173.73, 173.39, 173.39, 172.08, 172.08, 51.11, 51.11, 34.99, 34.99, 31.20, 31.20, 30.32, 30.32, 28.95, 28.95, 28.91, 28.91, 28.89, 28.89, 28.73, 28.73, 28.61, 28.61, 28.51, 28.51, 26.56, 26.56, 25.15, 25.15, 21.99, 21.99, 13.82, 13.82; FT-IR (ATR) ν_{max} (cm^{-1}) = 3309, 2937, 2914, 2848, 1730, 1714, 1701, 1651, 1624, 1543; MS (ESI): *m/z* = 414.3 $[MH]^+$, 436.3 $[M+Na]^+$, 827.6 $[2M+H]^+$, 849.6 $[2M+Na]^+$; elemental analysis calculated for $C_{23}H_{43}NO_5$: C, 66.79; H, 10.48; N, 3.39; found: C, 66.87; H, 10.45; N, 3.25.

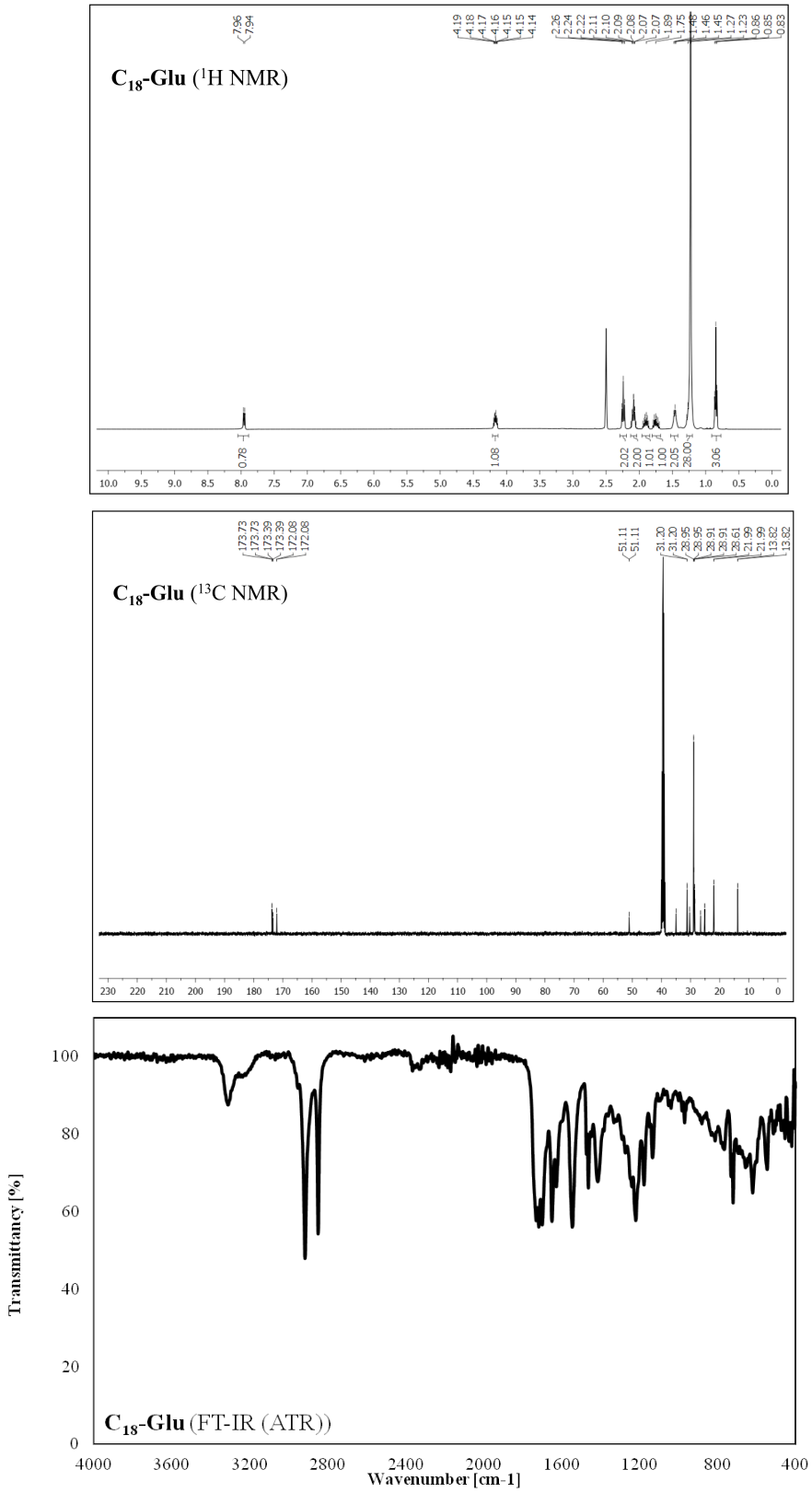

Fig. S3 ^{1}H NMR (top), ^{13}C NMR (middle) and FT-IR (bottom) spectra of **C_{18}-Glu**.

3.2. Synthesis and characterization of click-Glu

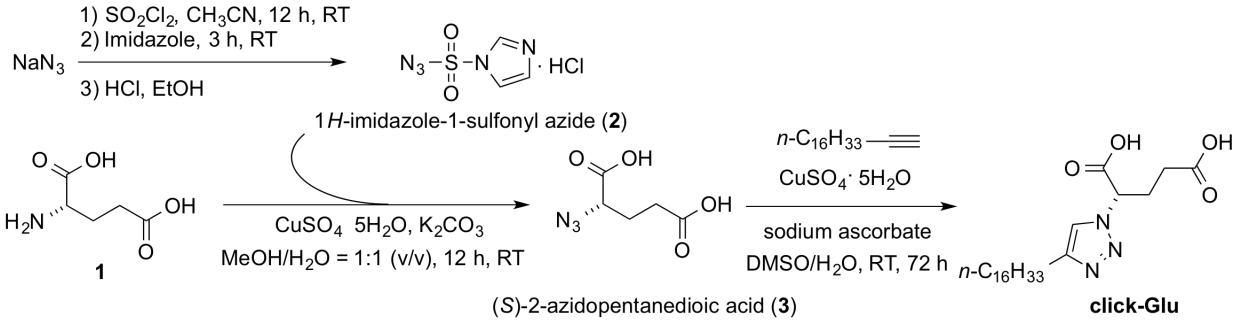

Scheme 2. Synthetic scheme for the preparation of **click-Glu**.

*(S)-2-Azidopentanedioic acid (**3**)*

1H-Imidazole-1-sulfonyl azide hydrochloride (**2**) (3.78 g, 18 mmol), prepared as previously described,[3] was added to a suspension of L-glutamic acid (**1**) (2.21 g, 15 mmol), anhydrous potassium carbonate (7.67 g, 55.5 mmol) and copper(II) sulfate pentahydrate (38 mg, 0.15 mmol) in methanol (75 mL). The reaction mixture was stirred overnight at room temperature. Then, the solvent was removed and the resulting residue was diluted with water (40 mL), acidified with conc. HCl (pH = 2) and extracted with ethyl acetate (3 × 40 mL). The combined organic phases were dried over anhydrous magnesium sulfate, filtered and concentrated. The resulting residue was purified by column chromatography (eluent: Et_2O/Hx/AcOH 49:50:1) affording the desired product as colorless oil in 67% yield (1.75 g, 10.1 mmol). Spectroscopic data were in agreement with those published.[12] $[\alpha]_D$ = –74.7 (*c* 0.43, $CHCl_3$). ^{1}H NMR (400 MHz, $CDCl_3$) d 9.76 (brs, 2H), 4.12 (dd, *J* = 7.8, 5.5 Hz, 1H), 2.66–2.53 (m, 2H), 2.29–2.18 (m, 1H), 2.16–2.06 (m, 1H) ppm (^{1}H NMR data are in agreement with those published[13]). ^{13}C NMR (100 MHz, $CDCl_3$) d 178.9, 176.1, 60.7, 29.7, 26.2 ppm. FT-IR (ATR) ν_{max} (cm^{-1}) 3450–2372, 2113, 1714, 1417. HRMS (ESI) Calcd. for $C_5H_6N_3O_4$ 172.0364; found 172.0360.

For cross-checking purposes the enantiomer (*R*)-azidopentanedioic acid ((*R*)-**3**) was also synthesized from D-glutamic acid using the same procedure: $[\alpha]_D$ = +76.5 (*c* 0.42, $CHCl_3$).

*(S)-2-(4-Hexadecyl-1H-1,2,3-triazol-4-yl)pentanedioic acid (**click-Glu**)*

To a stirred solution of octadec-1-yne (0.61 g, 2.40 mmol) and compound **1** (0.42 g, 2.40 mmol) in a 1:2 (v/v) mixture of DMSO/H_2O (2.5 mL) at RT were added 1M stock-solutions of $CuSO_4 \cdot 5H_2O$ (0.23 mL, 0.24 mmol) and sodium ascorbate (0.92 mL, 0.96 mmol). Due to a clear increase of viscosity after a short period of time, the total solvent volume was further increased to 10 mL. After stirring for 72 h, the solvent mixture was removed by lyophilization. The obtained residue was redissolved in a 1:1 (v/v) mixture of EtOAc/THF (50 mL) and washed with brine containing 0.1 M EDTA·Na_2 (2 × 50 mL), brine (2 × 25 mL) and water (3 × 25 mL) in order to remove most of organic and inorganic impurities. The organic layer was dried over Na_2SO_4, filtered and concentrated under reduced pressure. The obtained residue was recrystallized from acetone affording the title compound as a white solid in 87% yield (0.89 g, 2.09 mmol). ^{1}H NMR (400 MHz, DMSO-d_6) δ (ppm) = 7.94 (s, 1H), 5.35 (dd, *J* = 10.2, 5.2 Hz, 1H), 2.61 (t, *J* = 7.6 Hz, 2H), 2.47–2.35 (m, 1H), 2.37–2.23 (m, 1H), 2.20–1.99 (m, 2H), 1.59 (bs, 2H), 1.26 (s, 26H), 0.85 (t, *J* = 6.8 Hz, 3H); ^{13}C NMR (101 MHz, DMSO-d_6) δ (ppm) = 173.04, 169.96, 146.83, 121.57, 61.04, 31.19, 29.63, 28.94, 28.87, 28.77, 28.67, 28.60, 28.49, 26.46, 24.93, 21.99, 13.83; FT-IR (ATR) ν_{max} (cm^{-1}) = 3155, 2960, 2916, 2848, 1749, 1699, 1556; MS (ESI): *m/z* = 424.3 $[MH]^+$, 847.6 $[2M+H]^+$; elemental analysis calculated for $C_{23}H_{41}N_3O_5$: C, 65.22; H, 9.76; N, 9.92; found: C, 65.35; H, 9.70; N, 10.08.

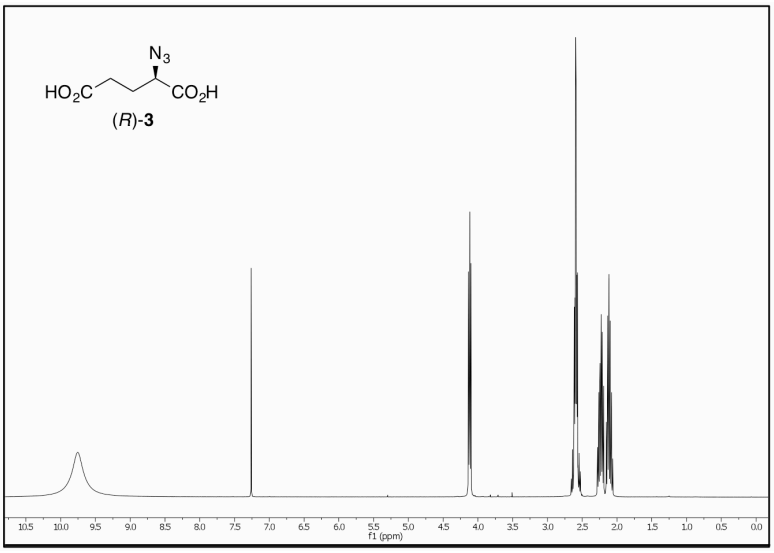
N3
HO2C
CO2H
(R)-3
10.5 10.0 9.5 9.0 8.5 8.0 7.5 7.0 6.5 6.0 5.5 5.0 4.5 4.0 3.5 3.0 2.5 2.0 1.5 1.0 0.5 0.0
f1 (ppm)

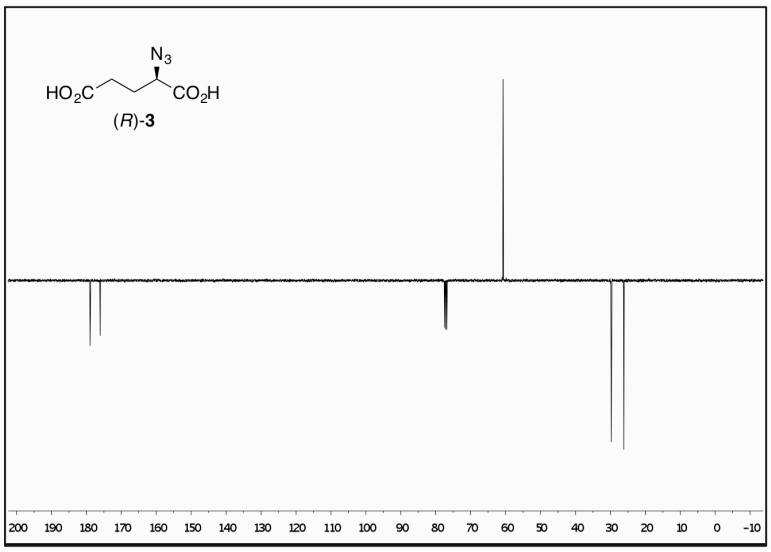
N3
HO2C
CO2H
(R)-3
200 190 180 170 160 150 140 130 120 110 100 90 80 70 60 50 40 30 20 10 0 -10

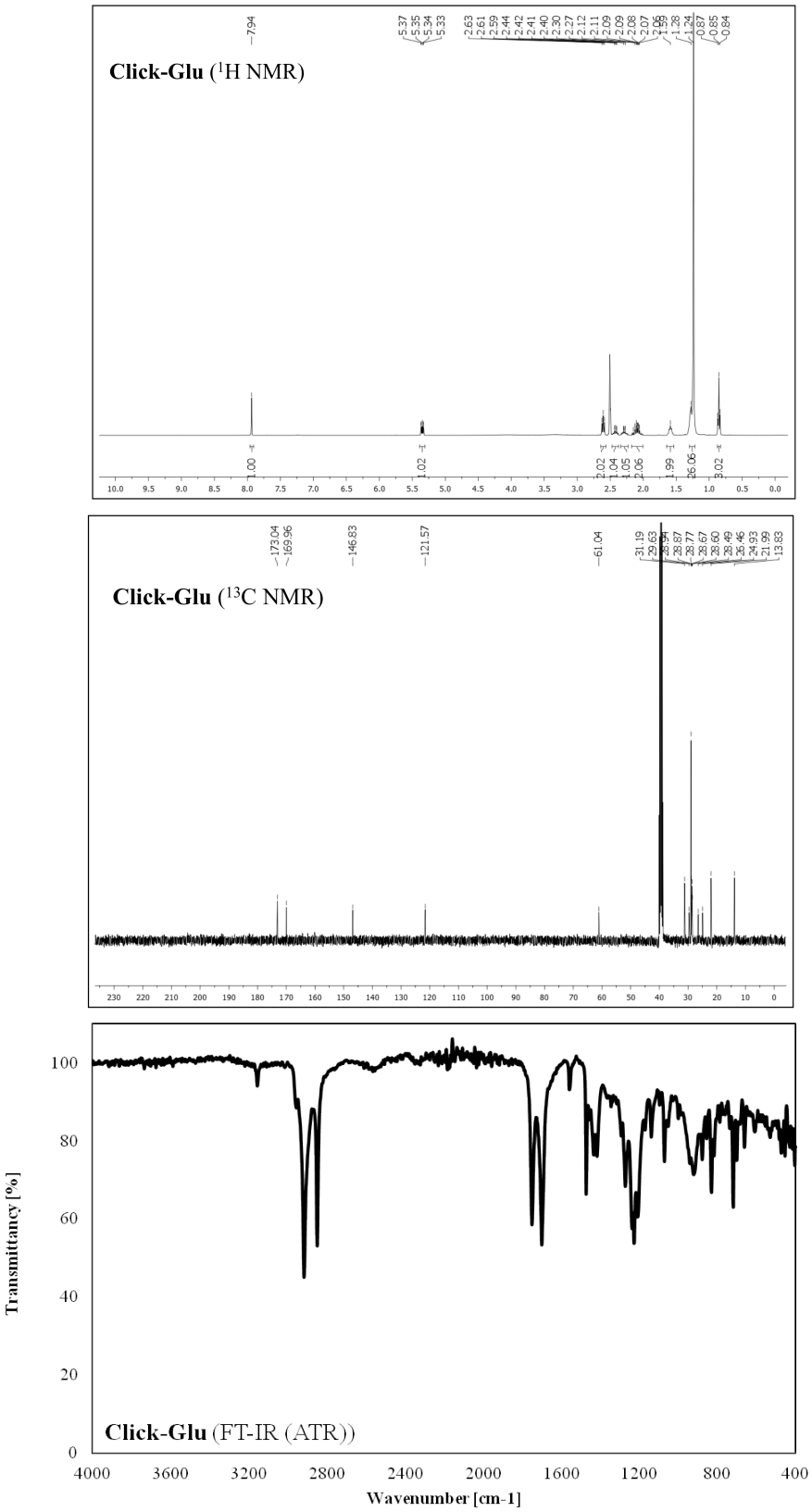

Fig. S4 ^{1}H NMR, ^{13}C NMR and FT-IR spectra of enantiopure intermediate **3** and **click-Glu**.

4. Preparation of gel materials

Typically, a weighted amount of the corresponding gelator and an appropriate solvent (0.5 mL) were placed into a screw-capped glass vial (4 cm length × 1 cm diameter) and gently heated with a heat gun until the solid material was completely dissolved. In some cases ultrasonication of the samples before heating could facilitate the dissolution of the compound. The resulting isotropic solution was then spontaneously cooled down to RT. No control over temperature rate during the heating-cooling process was applied. The material was preliminary classified as "gel" if it did not exhibit gravitational flow upon turning the vial upside-down at RT (Figure S5). The state was further confirmed by rheological measurements.

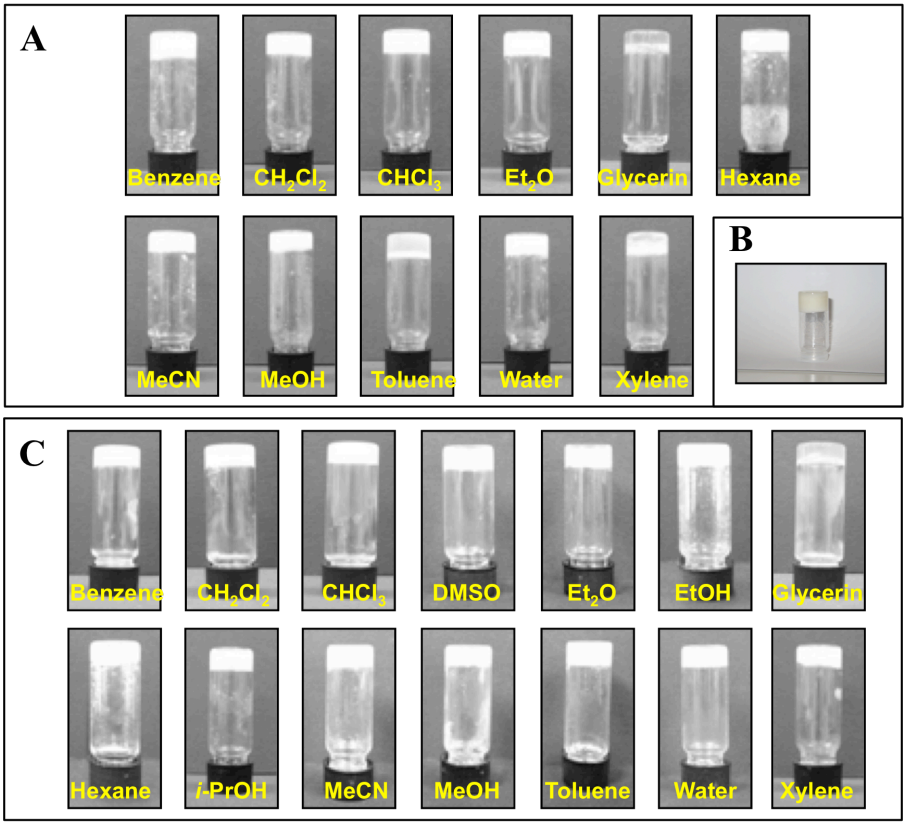

Fig. S5 Digital photographs of upside-down vials containing gels derived from compounds $\mathbf{C_{18}}$**-Glu** (**A**) and **click-Glu** (**C**) at the corresponding CGC in aqueous environment and various organic solvents as indicated in Table S1. **B**: Representative digital photograph showed *in situ* gelation of **click-Glu** during its synthesis in DMSO/water (2:1 v/v) at a concentration of ca. 200 g L^{-1}.

5. Gelation ability and gel properties (tabular data)

Tab. S1 Comparison of gelation ability and typical gel properties of **C_{18}-Glu** and **click-Glu** in aqueous environment and various organic media[a]

Solvent	**C_{18}-Glu**				**Click-Glu**			
	CGC ($g\ L^{-1}$)	Gel-Time (min)	T_{gel} (°C)	Appearance	CGC ($g\ L^{-1}$)	Gel-Time (min)	T_{gel} (°C)	Appearance
MeOH	33 ± 3	10 ± 1	41 ± 1	OG	25 ± 2	140 ± 20	51 ± 2	OG
EtOH	> 200	-	-	PG	72 ± 6	35 ± 5	46 ± 1	OG
i-PrOH	> 200	-	-	PG	180 ± 15	180 ± 30	38 ± 2	SG/OG
2-BuOH	> 200	-	-	PG	> 200	-	-	PG
1-Hexanol	> 200	-	-	P	> 200	-	-	PG
Glycerin	20 ± 2	1.5 ± 0.3	53 ± 1	TLG	12 ± 1	25 ± 5	55 ± 1	TLG
DMSO	> 200	-	-	P	180 ± 15	10 ± 1	41 ± 1	OG
DMF	> 200	-	-	P	> 200	-	-	P
CH_3CN	110 ± 10	2 ± 0.5	67 ± 2	OG	48 ± 4	5 ± 0.5	68 ± 2	OG
THF	> 200	-	-	CS	> 200	-	-	CS
Et_2O	18 ± 2	12 ± 3	61 ± 1	OG	78 ± 8	5 ± 0.5	49 ± 2	OG
EtOAc	> 200	-	-	P	> 200	-	-	P
CH_2Cl_2	100 ± 10	25 ± 5	53 ± 1	OG	180 ± 15	35 ± 5	40 ± 2	OG
$CHCl_3$	75 ± 8	8 ± 0.5	58 ± 2	OG	100 ± 10	7 ± 0.5	43 ± 2	OG
Xylenes	84 ± 8	1.5 ± 0.3	68 ± 1	OG	95 ± 15	0.5 ± 0.1	56 ± 1	OG
Benzene	175 ± 20	4.5 ± 0.5	73 ± 2	OG	200 ± 15	1.5 ± 0.3	64 ± 1	OG
Toluene	90 ± 10	2 ± 0.3	65 ± 1	OG	135 ± 10	0.5 ± 0.1	52 ± 1	OG
DOX	> 200	-	-	CS	> 200	-	-	CS
Acetone	> 200	-	-	P	> 200	-	-	P
n-Hexane	25 ± 2	5 ± 0.5	67 ± 2	OG	115 ± 10	0.5 ± 0.1	72 ± 2	OG
H_2O	25 ± 2	10 ± 0.5	47 ± 1	OG	17 ± 2	4.5 ± 0.3	61 ± 1	OG
PheCl	> 200	-	-	PG	> 200	-	-	PG
PheCN	> 200	-	-	PG	> 200	-	-	PG
IL	0.1–20	-	-	I	0.1–20	-	-	I
Olive oil	0.1–20	-	-	I	0.1–20	-	-	I
Silicon oil	0.1–20	-	-	I	0.1–20	-	-	I

[a] Error values reported as STDV were estimated from at least two randomized experiments. Abbreviations: CS = clear solution resulting after heating a mixture of the compound and the corresponding solvent; DOX = 1,4-dioxane; I = insolubility of the compound in the corresponding solvent; IL = 1-butyl-3-methylimidazolium hexafluorophosphate ($BMIM{\cdot}PF_6$; room temperature ionic liquid); OG = opaque gel; P = precipitation of the compound from isotropic solutions of compound and corresponding solvent (usually after 4–36 h); PG = partial gel (phase separation between gel and sol after time); PheCl = chlorobenzene; PheCN = benzonitrile; SG = soft gel (gravitational flow of the material after inversion of the test tube within 2 h); TLG = translucent gel.

Click-Glu exhibits a quite similar behaviour towards gelation in the tested solvents. Besides the formation of stable gels in the same solvents as **C_{18}-Glu** (sharing similar optical appearance) additional gelation of EtOH, *i*-PrOH and DMSO was observed extending the scope by 3 polar solvents.

Tab. S2 Evaluation of the accuracy of T_{gel} values determined using the customized set-up as described in Figure S2[a]

Entry	Compound	Solvent	Conc. (g L^{-1})	T_{gel} (°C)		
				IFM	DBM[d]	CM
1	**C_{18}-Glu**	H_2O	25	49 ± 1	49 ± 2	47 ± 1
2	**C_{18}-Glu**	$CHCl_3$	75	58 ± 1	56 ± 1	58 ± 2
3	**C_{18}-Glu**	Et_2O	18	57 ± 2	63 ± 1	61 ± 1
4	**C_{18}-Glu**[b]	CH_3CN	110	66 ± 2	64 ± 1	67 ± 2
5	**C_{18}-Glu**	Toluene	90	63 ± 1	63 ± 1	65 ± 1
6	**click-Glu**[b]	H_2O	17	62 ± 1	58 ± 2	61 ± 1
7	**click-Glu**	$CHCl_3$	100	42 ± 1	39 ± 2	43 ± 2
8	**click-Glu**	Et_2O	78	49 ± 2	48 ± 1	49 ± 2
9	**click-Glu**[b]	CH_3CN	48	67 ± 1	62 ± 2	68 ± 2
10	**click-Glu**	Toluene	135	52 ± 2	51 ± 1	52 ± 1
11	**A4**[c]	*i*-PrOH	19	54 ± 1	56 ± 1	51 ± 1
12	**A4**[c]	Toluene	20	40 ± 2	36 ± 2	40 ± 1
13	**A4**[c]	EtOH	70	51 ± 1	51 ± 1	53 ± 2

[a] Abbreviations: IFM = Inverse flow method.[10] DBM = dropping ball method.[14] CM = customized set-up. Error values reported as STDV were estimated from at least two randomized experiments. [b] The system has been investigated by DSC and T_{gel}-values were correlated with the first endothermic transition as indicated in Figure S7. [c] For comparative purposes known tetrapeptide gelator (**A4**)[15] in *i*-PrOH (19 g L^{-1}, T_{gel} = 52 °C determined by IFM and verified by correlation to the first transition in modulated DSC (56 ± 1 °C)), toluene (20 g L^{-1}, T_{gel} = 37 °C determined by IFM) and EtOH (70 g L^{-1}, T_{gel} = 52 °C determined by IFM) was also investigated. [d] Balls used for the determinations: 0.1 ± 0.02 mm diameter, 0.105 ± 0.010 g weight.

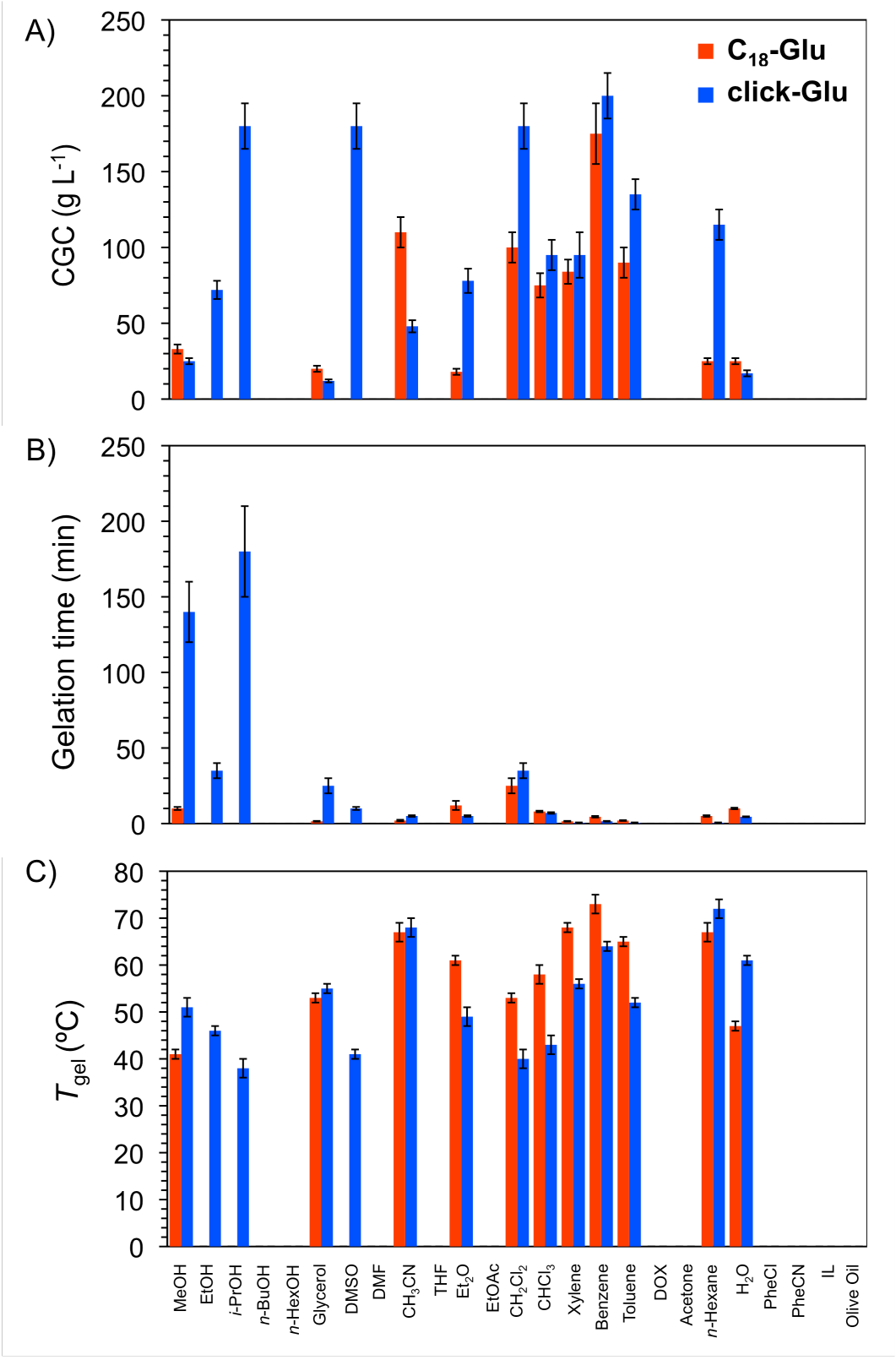

Fig. S6 Data from Table S1 represented as bar plots showing the differences in gelation properties of **C_{18}-Glu** and **click-Glu**. **A**) CGC values; **B**) gelation-time; **C**) T_{gel}-values. Abbreviations as indicated in Table S1.

6. Differential scanning calorimetry

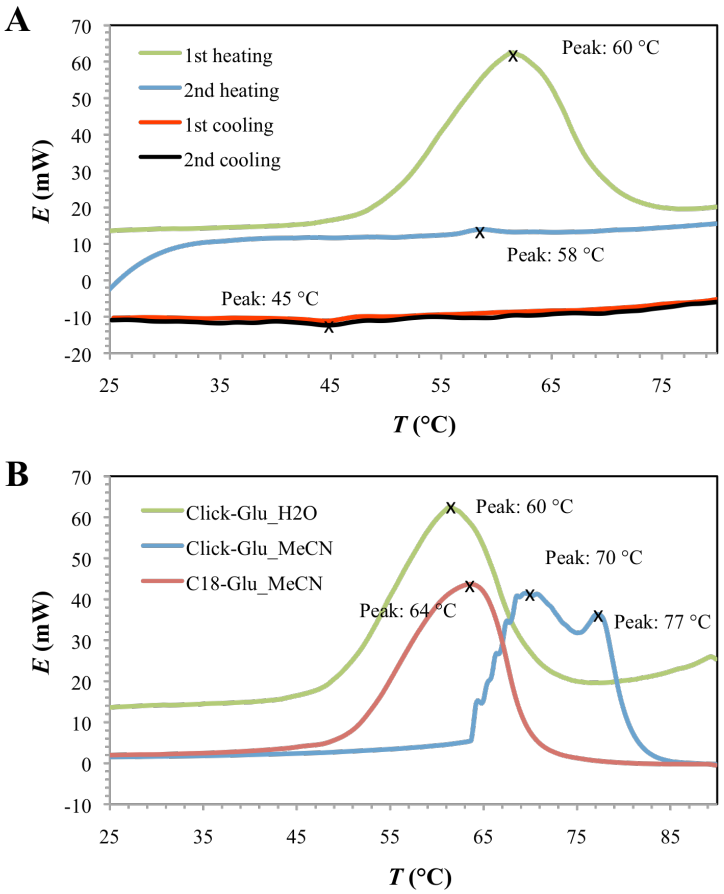

Fig. S7 A) Representative DSC spectrum of the gel made of **click-Glu** in H_2O (17 g L^{-1}). *Gel*-to-*sol* transition temperature (endothermic effect) was estimated in ca. 59 ± 1 ºC in two different cycles (first-order transition), which was in good agreement with the value obtained using IFM (T_{gel} = 62 ± 1 ºC) and the customized set-up (T_{gel} = 61 ± 1 ºC). On the other hand, *sol*-to-*gel* transition temperature (exothermic effect) was estimated in ca. 46 ºC due to thermal cycling hysteresis. B) Representative heating curves obtained by DSC of different gel-materials for T_{gel}-determinations at concentrations as indicated in Table S2. The observation of second order transition in gels from **click-Glu** in acetonitrile (48 g L^{-1}) could be an indication for cluster-formation of a different fibril assembly. In general the obtained values are in good agreement with experiments carried out in Table S2.

7. FT-IR spectra of gel and xerogel materials

Examining the powdered and xerogels states of materials derived from **C_{18}-Glu** in $CHCl_3$ and water significant differences could be found as illustrated in Figure S8. For materials made in $CHCl_3$, a clear shift in the amide-II band from 1544 cm^{-1} in the powdered state to 1539 cm^{-1} in the xerogel state was visible indicating that the amide NH-group forms H-bonds (this is confirmed also by a visible shift of the ν_{NH}-band from 3310 to 3332 cm^{-1}). The participation of amide CO-groups in H-bonding was suggested by a shift in the amide-I band from 1649 to 1644 cm^{-1}. No shift of the $\nu_{C=O}$ bands of the carboxylic acid-groups at 1730 and 1717 cm^{-1} indicated free, laterally H-bonded and bifurcated acid-groups, which are necessary for the formation of intra- and inter-layered H-bonds between intermolecular acid and/or amide groups. On the other hand, for materials made in water, the amide-II band was only slightly shifted in xerogel-state from 1544 to 1545 cm^{-1} indicating only a small participation of NH-groups in H-bonding (this is also supported by a marginal shift of the ν_{NH}-band from 3310 to 3311 cm^{-1}). No shift of the signals was observed for the amide-I band centered at 1644 cm^{-1}. Interestingly, $\nu_{C=O}$ bands of the carboxylic acid-groups centered at 1730 and 1717 cm^{-1} were significantly shifted to 1700 and 1689 cm^{-1} respectively, indicating a strong participation of the carboxylic acid moieties in H-bonding. These results are in agreement with **C_{18}-Glu** forming mainly intermolecular H-bonds in water, whereas both intra- and intermolecular H-bonds occur in $CHCl_3$. Examining powdered and gel-states of materials derived from **click-Glu** it is obvious that they behave in an opposite way as compared to materials based on **C_{18}-Glu**. For materials prepared in water, ν_{CH}-bands of the triazole moiety significantly shifted from 3155 to 3069 cm^{-1} indicating strong participation of the donor-H in H-bonding. Additionally, $\nu_{C=O}$ bands centered at 1749 and 1699 cm^{-1} were shifted towards 1733 and 1674 cm^{-1} respectively in the gel-state, indicating the participation of the carboxylic acid moieties in H-bonding. On the other hand, for materials made in $CHCl_3$, only little participation of the triazole H-donor was visible as indicated by a marginal shift from 3155 to 3154 cm^{-1}. Additionally, the strong $\nu_{C=O}$ bands were not shifted in comparison to the powdered state suggesting that **click-Glu** forms mainly intermolecular H-bonds in $CHCl_3$, whereas both types of H-bonding occur in water.

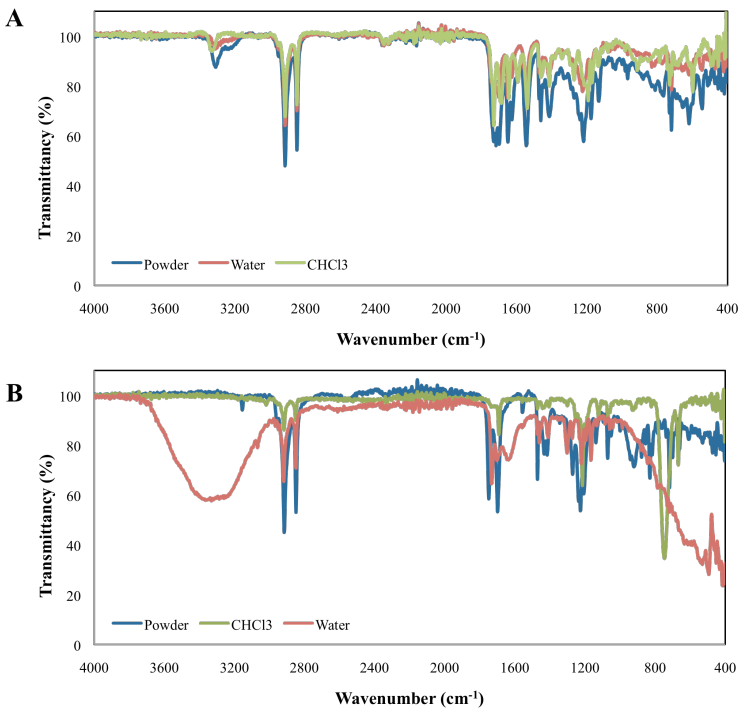

Fig. S8 Comparative FT-IR spectra: A) **C_{18}-Glu** as synthesized (powder) and xerogels derived from the corresponding gels in water and $CHCl_3$. B) **Click-Glu** as synthesized (powder) and gels made in water and $CHCl_3$.

8. Effect of gelator concentration on T_{gel} and gelation kinetics

A typical plateau region for all examples (ΔT_{gel} = 20–33 °C) was visible before the gels collapsed into partial and inhomogeneous gels with expelling some liquid on top over short periods of time (< 4 h).

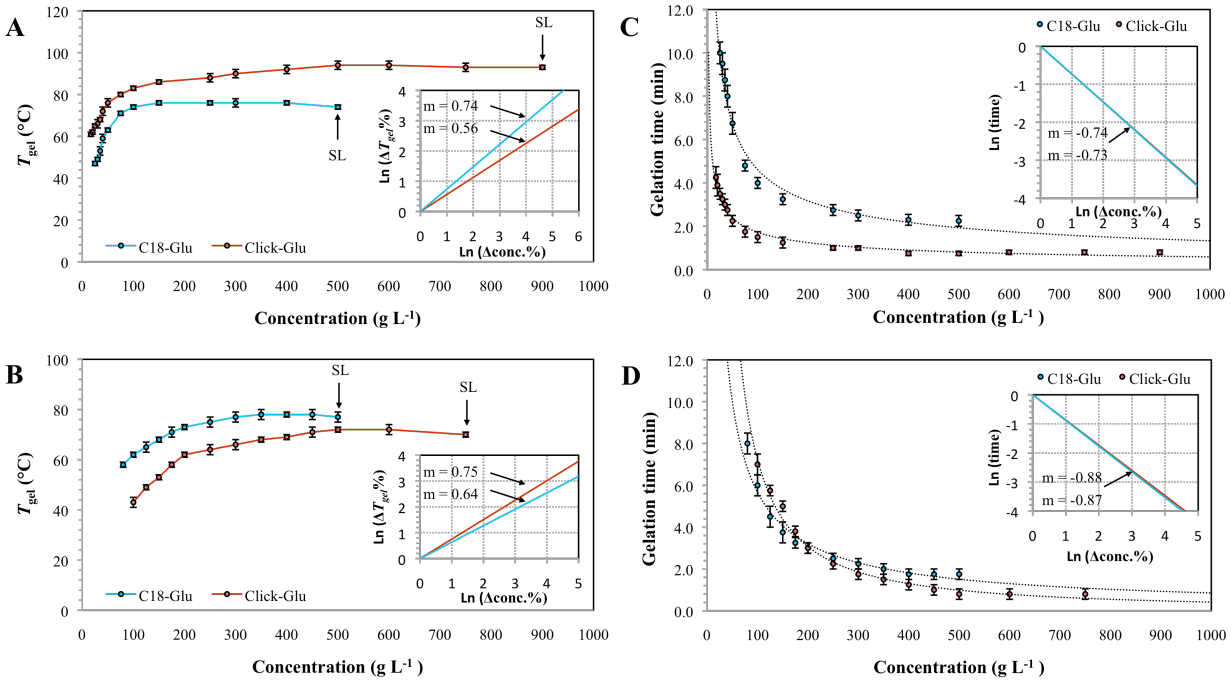

Fig. S9 A-B) Evolution of T_{gel} with increasing gelator concentration of gels made from **C_{18}-Glu** and **click-Glu** in (**A**) water and (**B**) $CHCl_3$. Inset-plots: Normalized Ln-Ln plots of the corresponding percentual increments. **C, D** Gelation kinetics of compounds **C_{18}-Glu** and **click-Glu** in (**C**) water and (**D**) $CHCl_3$. Inset-plots: Normalized Ln-Ln graphs of the gelation-time against percentual increments of concentration. Abbreviations: m = slope; SL = stability limit.

9. Stimuli-responsive behavior

All gel-materials full thermo-reversible behavior, regardless the gelator and the nature of the solvent, without any remarkable changes in T_{gel}-values even after several cycles of heating and cooling. Figure S10 summarizes the multi-responsive map of gels derived from **C_{18}-Glu** and **click-Glu**.

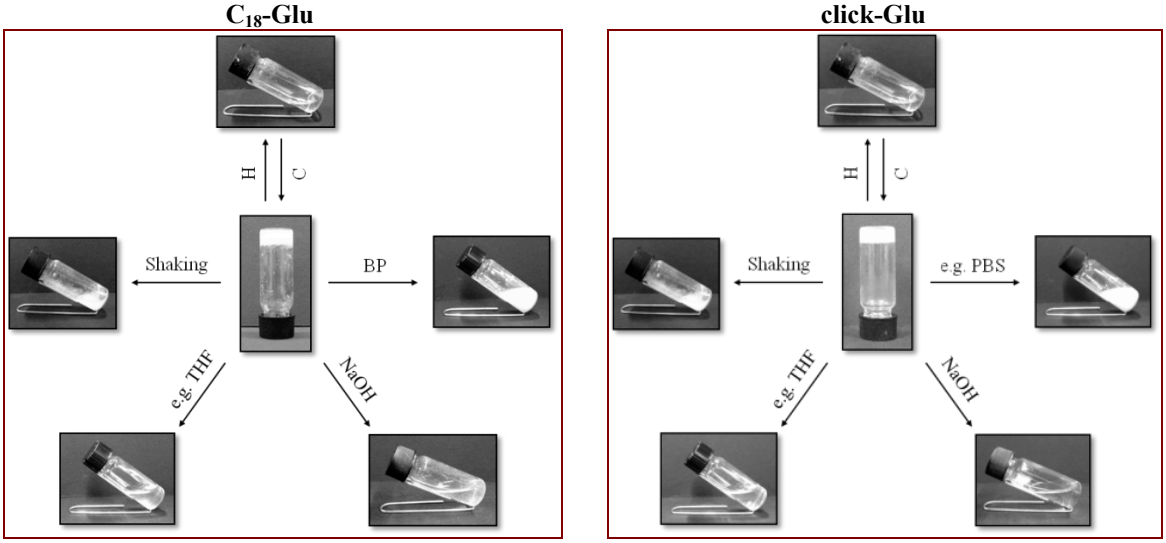

Fig. S10 *Left*: Representative diagram showing the multistimuli response of a gel derived from **C_{18}-Glu** in water (25 g L^{-1}). Abbreviations: C = cooling; H = heating; BP = borate buffer (pH = 9.2). *Right*: Representative diagram showing the preparation of multistimuli response of gels derived from **click-Glu** in water (17 g L^{-1}). Abbreviations: C = cooling; H = heating; PBS = phosphate buffered saline.

In the case of **click-Glu**, irreversible *gel*-to-*sol* phase transitions could be observed by mechanical agitation and addition of certain chemical substances. Gel-materials were dissolved in the presence of NaOH, while being stable towards neutral and acidic conditions. Also treatment with certain electrolytes (e.g., Na_2SO_4, NaCl, CsF), buffered solutions (phosphate buffer saline (PBS; pH = 7.4) and borate buffer (pH = 9.2)) and organic solvents (i.e., THF, 1,4-dioxane) resulted in phase transition. Response towards metal-ions (i.e., Ag^{+}, Cu^{2+}, Fe^{3+} and Ce^{4+}), halides (i.e., TBACl, TBAB, TBAF), other organic solvents (i.e., *n*-hexane, toluene, cyclohexane, EtOAc, MeCN, MeOH, DMSO, DMF, acetone, CH_2Cl_2), ultrasound treatment or UV-irradiation was not be observed. Gels derived from **click-Glu** in $CHCl_3$ behaved approximately the same, as also gels derived from **C_{18}-Glu** in both water and $CHCl_3$, except from being stable against electrolytes and PBS-buffered solutions. In general the response towards external stimuli was quite fast being in a range between 30–240 min resulting in complete dissolution or collapse of the gel phases.

It is important mentioning that the use of higher concentration of gelator enhanced the stability of the gel phases towards buffered solutions. Thus, at concentrations up to 60 g L^{-1} no major degradation of the gel was observed neither with **click-Glu** nor with **C_{18}-Glu**. These conditions were used for the preliminary studies of drug release (*vide infra*). Nevertheless, the fact that the gel phase can undergo slow degradation over time at a certain concentration could also be used in favor of the development of other drug delivery systems.

10. Additional electron microscopy images

Xerogels obtained from the corresponding gels made of **C_{18}-Glu** or **click-Glu** at comparable concentrations showed remarkable morphological differences. Obviously, different patterns of interactions between gelator molecules and gelator-solvent molecules should contribute to such differences. Besides H-bonding and van der Waals interactions as major driving-forces for the gelation process in both cases, potential π-π-stacking should be also considered in the case of **click-Glu**. Thus, considering the differences on the gelation abilities and gel properties, the role of the triazole ring is clearly beyond its classical consideration solely as a linker. Nevertheless, the eventual generation of artifacts during SEM/TEM imaging is always possible due to sample preparation. For this reason, cryo-imaging techniques are generally more appropriate to study these types of materials. The high aspect ratio of the entangled networks is a consequence of a strong anisotropic growth process, which indicates a well-ordered molecular packing to form the unit nanostructures.

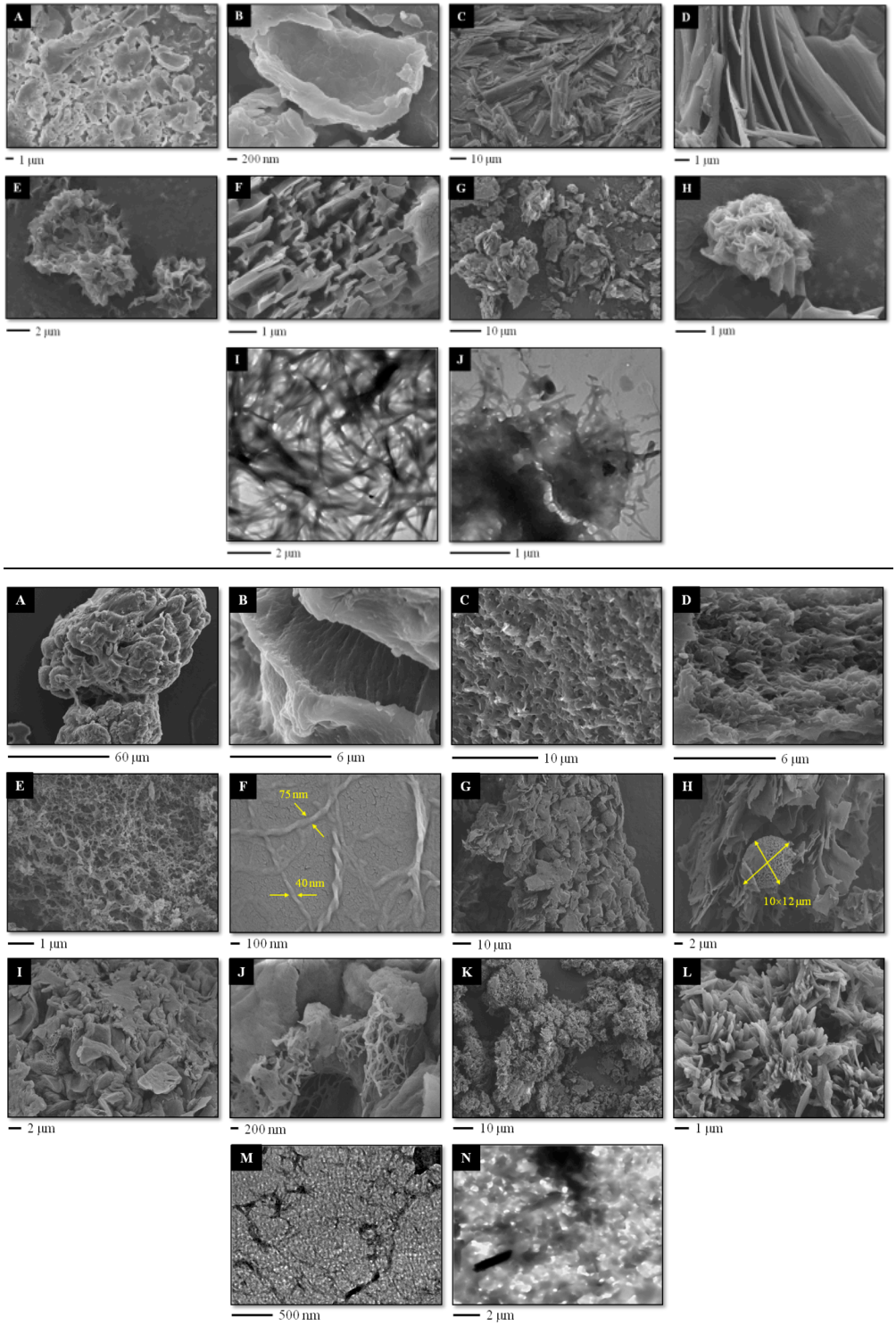

Fig. S11 *Top*: FESEM (**A-H**) and TEM (**I-J**) images of xerogels prepared by the freeze-drying method of materials derived from **C_{18}-Glu** and **Click-Glu** at comparable concentrations. **A, B, I**: **C_{18}-Glu** in water (25 g L^{-1}); **C, D**: **C_{18}-Glu** in $CHCl_3$ (100 g L^{-1}); **E, F, J**: **Click-Glu** in water (25 g L^{-1}); **G, H**: **Click-Glu** in $CHCl_3$ (100 g L^{-1}). *Bottom*: Additional SEM (**A-D**), FESEM (**E-L**) and TEM (**M-N**) images of xerogels prepared by the freeze-drying method of materials derived from **C_{18}-Glu** and **Click-Glu** at comparable concentrations. **A, B, M**: **C_{18}-Glu** in toluene (135 g L^{-1}); **C, D, N**: **Click-Glu** in toluene (135 g L^{-1}); **E, F**: **C_{18}-Glu** in MeCN (110 g L^{-1}); **G, H**: **Click-Glu** in MeCN (100 g L^{-1}); **I, J**: **C_{18}-Glu** in Et_2O (78 g L^{-1}); **K, L**: **Click-Glu** in Et_2O (78 g L^{-1}).

11. Gas adsorption measurements

Low-pressure gas adsorption measurements (up to 1 bar) were performed on a Quantachrome Quadrasorb automatic volumetric instrument at 77 K using N_2 gas. Xerogels of the compounds were obtained from hydrogels (25 g L^{-1}) by the freeze-drying method. Both materials are able to reversibly uptake N_2 indicating pore-sizes of bigger than the kinetic diameter of N_2 (3.6 Å). Materials derived from **C_{18}-Glu** can uptake up to 35.7 mmol g^{-1} (207.2 cm^3 g^{-1} at 77 K) N_2, whereas materials based on **click-Glu** can uptake 6.2 mmol g^{-1} (36.0 cm^3 g^{-1} at 77 K) at 1 bar pressure, which is in good agreement with the determined surface areas of 53.4 and 22.6 m^2 g^{-1} respectively. Gas-adsorption and desorption plots are illustrated in Figure **S12**.

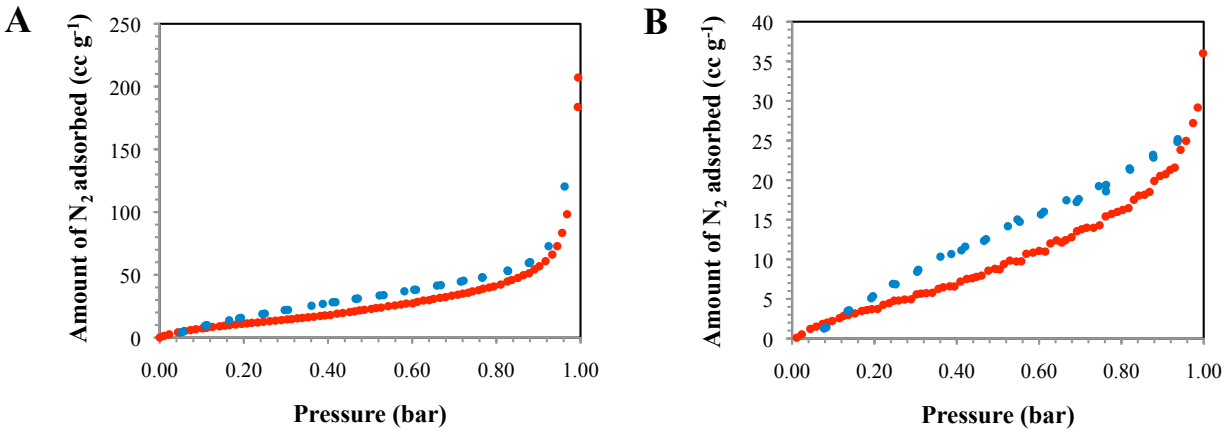

Fig. S12 N_2-adsorption isotherms below 1.0 bar for xerogels derived from hydrogels of **C_{18}-Glu** (**A**) and **Click-Glu** (**B**) with comparable concentrations (25 g L^{-1}). Red and blue circles represent adsorption and desorption respectively.

12. Rheological measurements

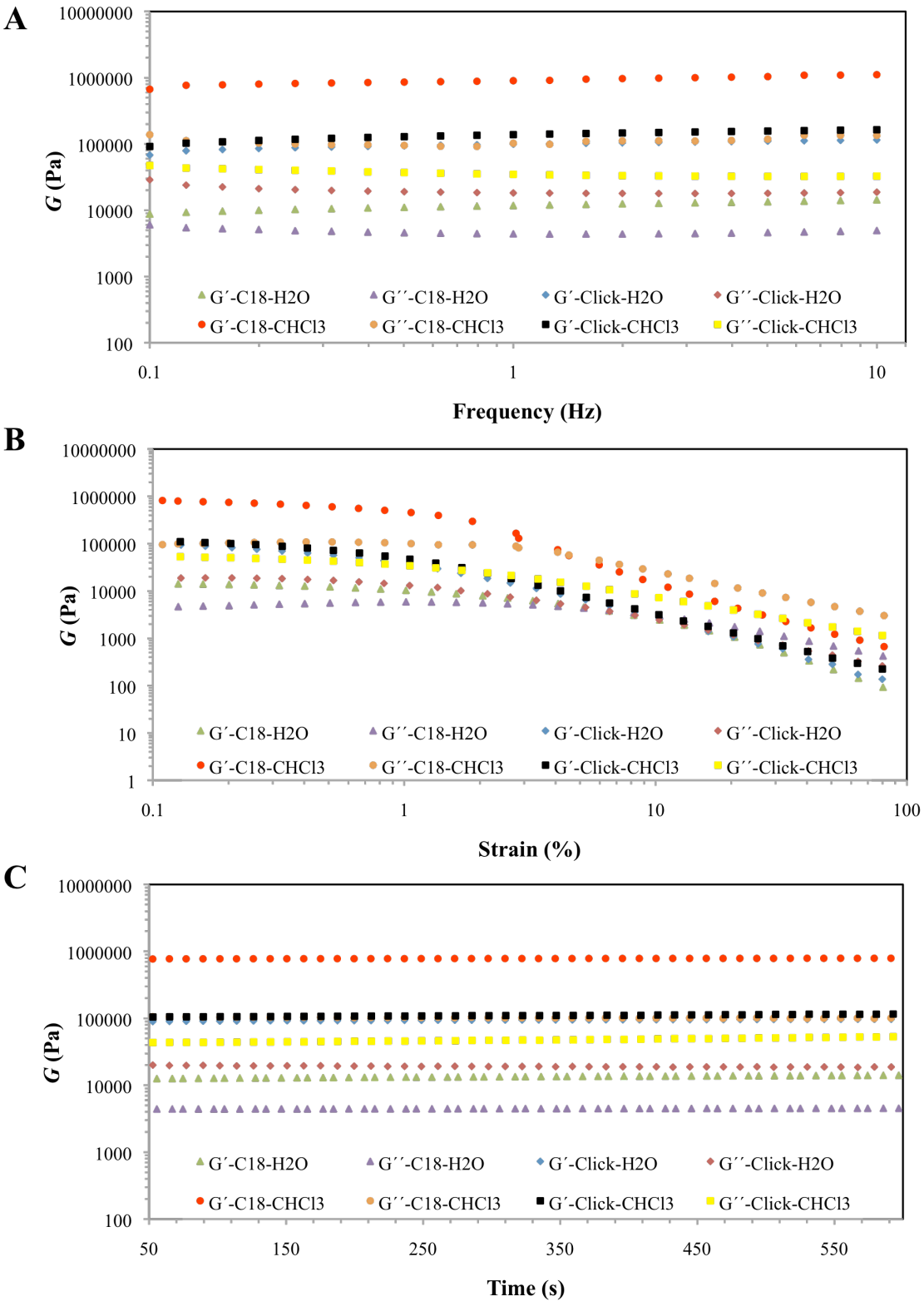

Fig. S13 Oscillatory rheological experiments of model gels prepared from **C_{18}-Glu** and **click-Glu** in water (25 g L^{-1}) and $CHCl_3$ (100 g L^{-1}). **A**: DFS-plots. **B**: DSS-plots. **C**: DTS-plots.

13. Potential models for self-assembly

The formation of distinctive nanostructures could be explained by different H-bonding patterns caused by either polar protic or non-polar environments. Thus, protic environments apparently favor the assembly of **C_{18}-Glu** in molecular multilayers resembling nanoalmond crunch mainly due to intermolecular H-bonding between the amide NH-bond and the CO-group of the acid moiety next to the chiral centre, whereas non-polar solvents lead to the formation of nanofibers in which both inter- and intramolecular H-bonding are nearly equally important. The opposite tendency was observed for **click-Glu**, suggesting that the isosteric replacement can be used to trigger the formation of desired nanostructures in specific solvents (Figure S14). Evidences of such divergent assembly mechanisms of the two isosteres associated to different H-bonding arrangements depending on the solvent nature were also obtained from FT-IR measurements using H_2O and $CHCl_3$ as model solvents (see section 7).

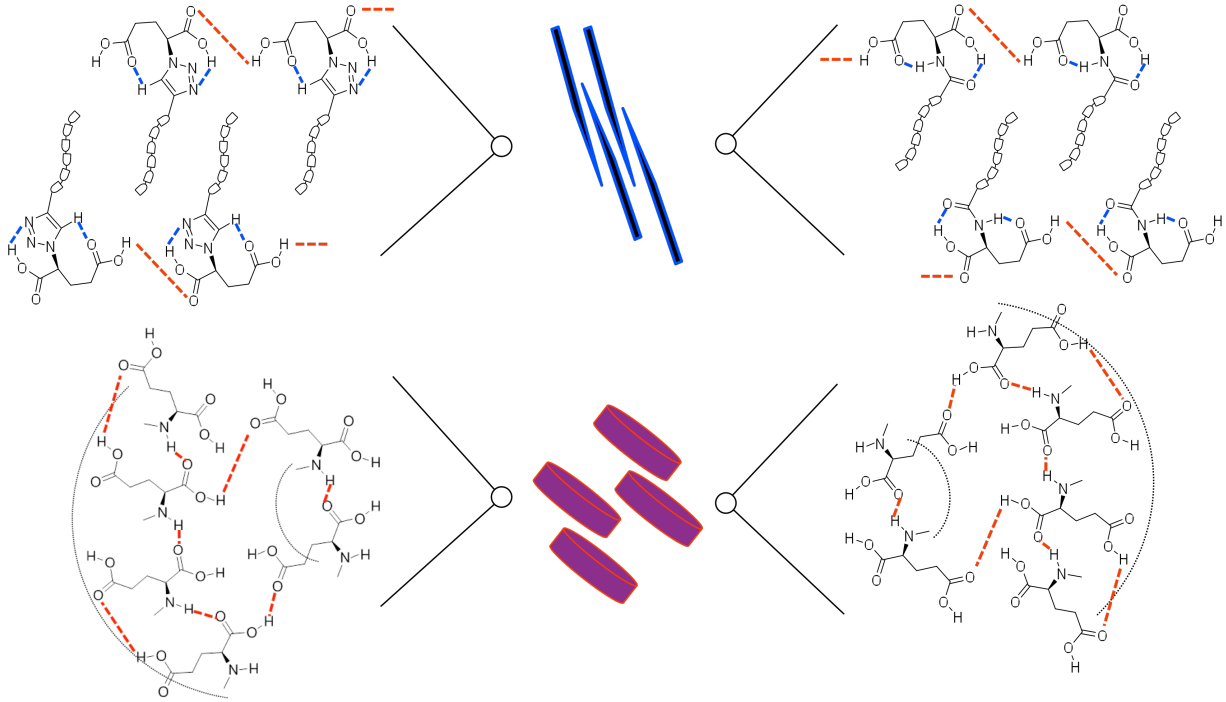

Fig. S14 Plausible models of favored H-bonded self-assembly of **C_{18}-Glu** and **Click-Glu** into lamellar or almond-like nanostructures, which can be modulated by the solvent nature. Red dashed lines indicate intermolecular H-bonding and blue dashed lines indicate intramolecular H-bonding. The proposed potential gelation mechanisms are based on previous studies,[11] FT-IR and preliminary temperature-controlled NMR data, as well as the isosteric nature of amides and 1,2,3-triazoles.

14. Drug release studies

Vancomycin is a type of glycopeptide antibiotic and used in the treatment of infections caused by Gram-positive bacteria. It is one of the rare natural haloorganic compounds and was first isolated in 1953.[16] Hydrophilic drugs like vancomycin are known to predominately distribute into the solvent phase rather than in the gel resulting in a relative quick and mostly complete release during drug release experiments, which makes this type of drug very interesting for potential application.[17] Soft nature of supramolecular gel materials and the possibility to coassembly different, but structurally related, gelator molecules may constitute a key advantage with respect to conventional hard non-hydrogel materials like PLGA or hydroxyapatite.[18] In our studies, the gel phases remained stable (only tiny amounts of gel material were observed to separate from the bulk phase in some cases and no dissolution of the gel phase was observed).

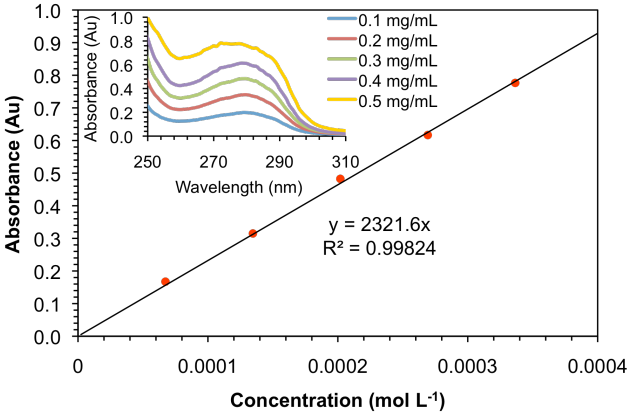

Fig. S15 Vancomycin-release calibration curve in the presence of PBS. Absorbance values of PBS and degraded gel materials at a max concentration of 25 mg/L were negligible at the max absorbance of the drug (280 nm).

Note: When working with vancomycin as model drug it is important to consider that solutions of vancomycin solutions in phosphate-buffered saline at 37 ºC has shown approximately 50% loss of the drug over 10 days of incubation due to its thermal degradation. This observation has been supported by HPLC and microbiological assay.[19]

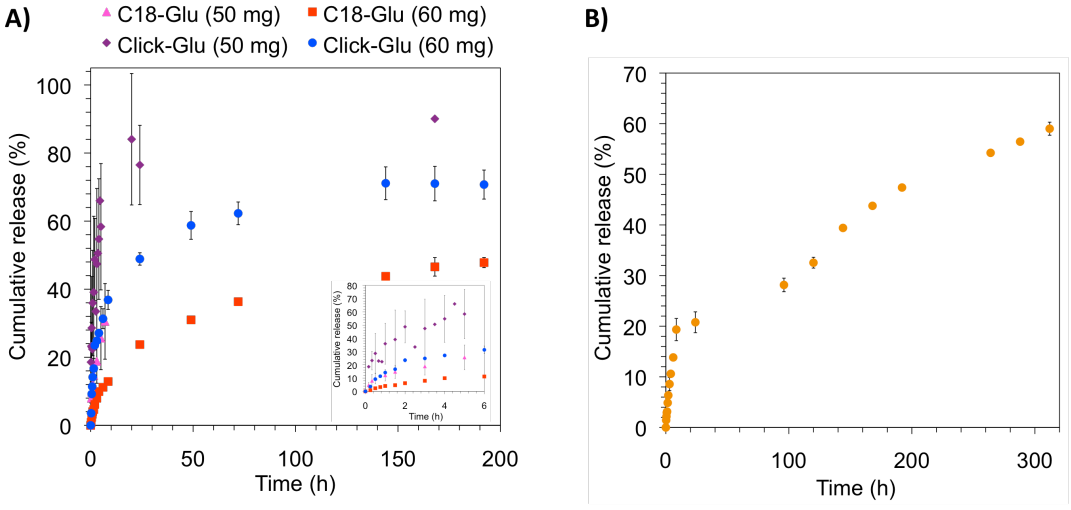

Fig. S16 A) Effect of the gelator concentration on the release of vancomycin from hydrogels made of **click-Glu** and **C_{18}-Glu**. B) Slow release of vancomycin from a hydrogel prepared using **click-Glu**:**C_{18}-Glu** (1:1, w/w). A plateau is observed after 300 h. Note: Partial fragmentation of the bulk gel was observed in this case, which could be also responsible to a certain extend of the complex release curve. On the other hand, a proper coupling of the dissolution

process of the gel matrix with the drug release constitutes also a promising approach for the development of sustained drug release systems.

In general, differences in the interaction patterns between solvent-gelator, gelator-gelator and gelator/fibril-drug molecules are expected to strongly influence the release kinetics of any entrapped drug. In order to demonstrate the versatility of these amphiphilic gels towards the entrapment and further release of other drugs with very different hydrophilic/hydrophobic balance, experiments with various anticancer drugs (i.e., methotrexate, camptothecin and flutamide) were also performed using hydrogels derived from **C_{18}-Glu** or **click-Glu** (Figure S17).

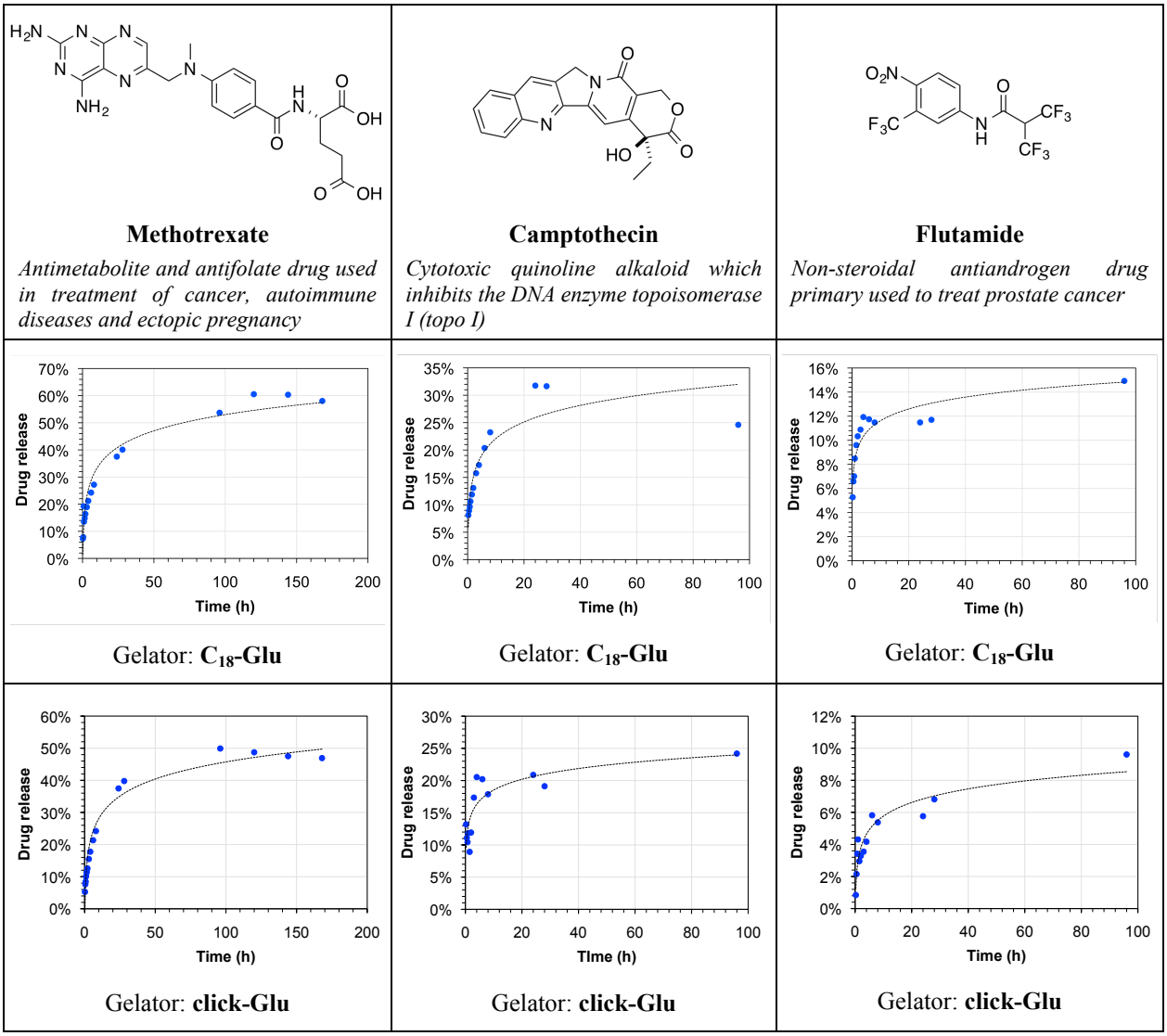

Fig. S17 Structures, description and preliminary release profiles of methotrexate, camptothecin and flutamide entrapped in hydrogels derived from **C_{18}-Glu** or **click-Glu**.

15. Antimicrobial studies

The Zone of Inhibition Test, also called Kirby-Bauer Test, is used clinically to qualitatively measure antibiotic resistance and industrially to test the ability of specimens to inhibit microbial growth.

Preparation of agar plates: A solution of 1% peptone, 0.5% yeast, 0.2% glucose and 1.5% of agar-agar (w/v) in milli-Q water was autoclaved at 120 °C for 20 min and then shaken. After cooling down to 95 °C, a Petri dish (8.5 cm diameter) was filled to half of the volume (ca. 25 mL). The dishes were shaken circularly on the bench to bring air bubbles to the edge. After cooling to room temperature, the plates were placed upside down to avoid condensed water to drop on the medium and stored in the refrigerator at 2-8 °C.

Hydrogels preparation: An aqueous vancomycin solution (1 mL from a 2 M solution) was added to a screw-capped vial containing either **C_{18}-Glu** or **click-Glu** (60 mg). The mixture was heated until complete dissolution of the material, transferred to a 2 mL syringe with cut cap and rested over night to obtain the corresponding stable hydrogels.

Antimicrobial tests with hydrogel pieces: *S. aureus* was seeded out evenly with a cotton bud on agar medium. Gel pieces of ca. 4 mm length and 9 mm diameter (0.25 mL) were placed on the bacteria plates. The plates were stored at 37 °C for 17 h.

Release of vancomycin from the hydrogels: An aqueous vancomycin solution (1 mL from a 2 M solution) was added to a screw-capped vial containing either **C_{18}-Glu** or **click-Glu** (60 mg). The mixture was heated until complete dissolution of the material and rested over night to obtain the corresponding hydrogels. The loaded-hydrogels were overlaid with PBS buffer (1 mL) and rested for additional 24 h.

Note: In the case of the hydrogel made of **click-Glu** without drug, a small inhomogeneous area of inhibition around the specimen was visible. Further detailed studies will focus on this observation.

Antimicrobial tests with drug release supernatants: *S. aureus* was seeded out evenly with a cotton bud on agar medium. Three samples of filter papers were soaked separately in 20 µL of (a) supernatant obtained from the drug release experiment, (b) pure PBS and (c) aqueous vancomycin solution (2M). The specimens were placed on the plates and stored at 37 °C for 17 h (Figure S18).

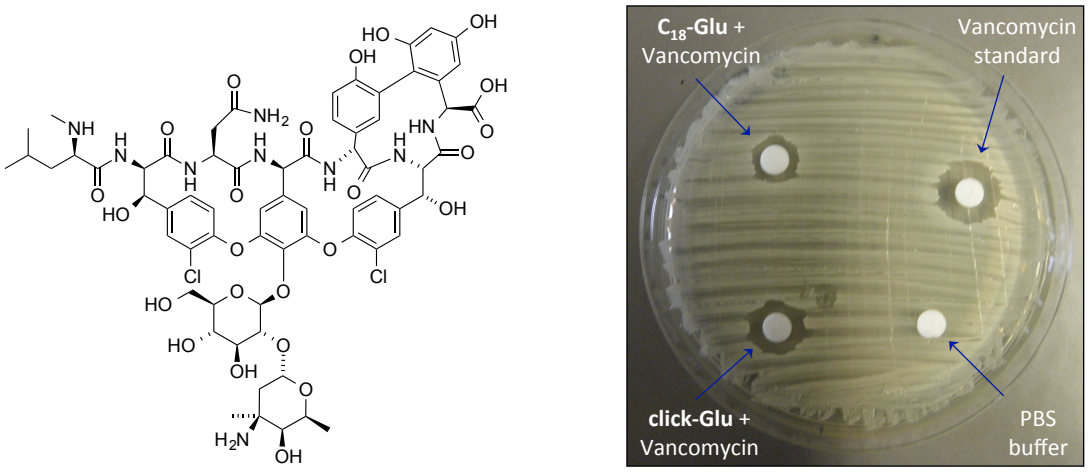

Fig. S18 *Left*: Chemical structure of vancomycin. *Right*: Zone of inhibition test against *S. aureus* for vancomycin after released from the hydrogel scaffolds. Clear inhibition zones around the specimens [**click-Glu** + vancomycin] (12 mm), [**C_{18}-Glu** + vancomycin] (10.5 mm) and vancomycin standard (13.5 mm) were observed. In agreement with the results obtained with the gel samples, a faster release from **click-Glu** compared to **C_{18}-Glu** was confirmed. No inhibition zone was observed for control PBS.

16. References

1 a) S. K. Thompson, A. M. Eppley, J. S. Frazee, M. G. Darcy, R. T. Lum, T. A. Tomaszek, L. A. Ivanhoff, J. F. Morris, E. J. Sternberg, D. M. Lambert, A. V. Fernandez, S. R. Petteway, T. D. Meek, B. W. Metcalf and J. G. Gleason, *Bioorg. Med. Chem. Lett.*, 1994, **4**, 2441; b) G. C. Tron, T. Pirali, R. A. Billington, P. L. Canonico, G. Sorba and A. A. Genazzani, *Med. Res. Rev.*, 2008, **28**, 278; c) Y. L. Angell and K. Burgess, *Chem. Soc. Rev.*, 2007, **36**, 1674; d) M. Corredor, J. Bujons, M. Orzáes, M. Sancho, E. Peréz-Payá, I. Alfonso and A. Messeguer, *Eur. J. Med. Chem.*, 2013, **63**, 892; e) G. Appendino, S. Bacchiega, A. Minassi, M. G. Cascio, L. De Petrocellis and V. Di Marzo, *Angew. Chem. Int. Ed.*, 2007, **119**, 9472; f) A. Tam, U. Arnold, M. B. Soellner and R. T. Raines, *J. Am. Chem. Soc.*, 2007, **129**, 12670; g) D. J. Pedersen and A. Abell, *Eur. J. Org. Chem.*, 2011, **13**, 2399; h) A. Brik, J. Alexandratos, Y.-C. Lin, J. H. Elder, A. J. Olson, A. Wladower, D. S. Goodsell and C. H. Wong, *Chem. Bio. Chem.*, 2005, **6**, 1167; i) J. M. Holub and K. Kirshenbaum, *Chem. Soc. Rev.*, 2010, **39**, 1325; j) V. D. Bock, D. Speijer, H. Hiemstra and J. H. van Maarseveen, *Org. Biomol. Chem.*, 2007, **5**, 971.

2 a) J. E. Moses and A. D. Moorhouse, *Chem. Soc. Rev.*, 2007, **36**, 1249; b) M. Juricek, P. H. J. Kouwer and A. E. Rowan, *Chem. Commun.*, 2011, **47**, 8740; c) A. J. Dirks, J. J. L. M. Cornelissen, F. L. van Delft, J. C. M. van Hest, R. J. M. Nolte, A. E. Rowan and F. P. J. T. Rutjes, *QSAR Comb. Sci.*, 2007, **26**, 1200.

3 a) J. J. Bryant and U. H. F. Bunz, *Chem. Asian J.*, 2013, **8**, 1354; b) Y. H. Lau, P. J. Rutlegde, M. Watkinson and M. H. Todd, *Chem. Soc. Rev.*, 2011, **40**, 2848.

4 a) J.-S. Qin, D.-Y. Du, W.-L. Li, J.-P. Zhang, S.-L. Li, Z.-M. Su, X.-L. Wang, Q. Xu, K.-Z. Shao and Y.-Q. Lan, *Chem. Sci.*, 2012, **3**, 2114; b) S. Wang, T. Zhao, G. Li, L. Wojtas, Q. Huo, M. Eddaoudi and Y. Liu, *J. Am. Chem. Soc.*, 2010, **132**, 18038; c) R.-B. Lin, D. Chen, Y.-Y. Lin, J.-P. Zhang and X. M. Chen, *Inorg. Chem.*, 2012, **51**, 9950.

5 For selected articles view: a) A. Hemamalini, T. M. Das, *New J. Chem.* **2013**, *37*, 2419; b) H.-F. Chow, C.-M.-Lo, Y. Chen, *Top. Heterocycl. Chem.* **2012**, *28*, 137; c) K. Ghosh, A. R. Sarkar and A. P. Chattopadhyay, *Eur. J. Org. Chem.*, 2012, **7**, 1311; d) K. Kuroiwa, T. Shibata, A. Takada, N. Nemoto and N. Kimizuka, *J. Am. Chem. Soc.*, 2004, **126**, 2016; e) R. T. Chen, S. Marchesan, R. A. Evans, K. E. Styan, G. K. Such, A. Postma, K. M. McLean, B. W. Muir and F. Caruso, *Biomacromolecules*, 2012, **13**, 889; f) G. Ghini, L. Lascialfari, C. Vinattieri, S. Cicchi, A. Brandi, D. Berti, F. Betti, P. Baglioni and M. Mannini, *Soft Matter*, 2009, **5**, 1863; g) D. D. Díaz, J. J. M. Tellado, D. G. Velázquez, A. G. Ravelo, *Tetrahedron Lett.*, 2008, **49**, 1340; h) J. Zhang, H.-F. Chow, M.-C. Chan, G. K.-W. Chow and D. Kuck, *Chem. Eur. J.*, 2013, **19**, 15019; i) D. Liu, D. Wang, M. Wang, Y. Zheng, K. Koynov, G. K. Auernhammer, H. J. Butt and T. Ikeda, *Macromolecules*, 2013, **46**, 4617; j) V. Bhalla, H. Singh, M. Kumar and S. K. Prasad, *Langmuir*, 2011, **27**, 15275; k) S. M. Park, Y. S. Lee and B. H. Kim, *Chem. Commun.*, 2003, **23**, 2912; l) A. Hemamalini and T. M. Das, *New J. Chem.*, 2013, **37**, 2419; m) O. Roubeau, A. Colin, V. Schmitt and R. Clérac, *Angew. Chem. Int. Ed.*, 2004, **43**, 3283-3286; n) R. M. Meudtner and S. Hecht, *Macromol. Rapid Commun.*, 2008, **29**, 347; o) J. P. Byrne, J. A. Kitchen, O. Kotova, V. Leigh, A. P. Bell, J. J. Boland, M. Albrecht and T. Gunnlaugsson, *Dalton Trans.*, 2014, **43**, 196; p) X. Yan, D. Xu, X. Chi, J. Chen, S. Dong, X. Ding, Y. Yu, F. Huang, *Adv. Mater.*, 2012, **24**, 362; q) S.-L. Yim, H.-F. Chow, M.-C. Chan, C.-M. Che and K.-H. Low, *Chem. Eur. J.*, 2013, **19**, 2478; r) J. Yuan, H. Zhang, G. Hong, Y. Chen, G. Chen, Y. Xu and W. Weng, *J. Mater. Chem. B*, 2013, **1**, 4809; s) J. Yuan, X. Fang, L. Zhang, G. Hong, Y. Lin, Q. Zheng, Y. Xu, Y. Ruan, W. Weng, H. Xia and G. Chen, *J. Mater. Chem.*, 2012, **22**, 11515; t) N.-T. Huynh, Y.-S. Jeon, M. Zrinyi and J.-H. Kim, *Polym. Int.*, 2013, **62**, 266; u) D. D. Díaz, K. Rajagopal, E. Strable, J. Schneider and M. G. Finn, *J. Am. Chem. Soc.*, 2006, **128**, 6056.

6 D. Derossi, Y. Kajiwara, Y. Osada, *Polymer Gels: Fundamentals and Biomedical Applications*, Plenum Press, New York, 1991, and references therein; b) J. H. Jung, S. Shinkai, *Top. Curr. Chem.*, 2004, **248**, 223; c) N. M. Sangeetha, U. Maitra, *Chem. Soc. Rev.*, 2005, **34**, 821; d) R. V. Ulijn, A. M. Smith, *Chem. Soc. Rev.*, 2008, **37**, 664; e) M. O. M. Piepenbrock, G. O. Lloyd, N. Clarke, J. W. Steed, *Chem. Rev.*, 2010, **110**, 1960; f) D. D. Diaz, D. Kuhbeck, R. J. Koopmans, *Chem. Soc. Rev.*, 2011, **40**, 427.

7 For reviews see: a) B. Jeong, S. W. Kim and Y. H. Bae, *Adv. Drug Deliv. Rev.*, 2002, **54**, 37; b) M. Goldberg, R. Langer and X. Jia, *J. Biomat. Sci.*, 2007, **18**, 241; c) N. A. Peppas, *J. Bioact. Compat. Pol.*, 1991, **6**, 241; d) H. J. Chung and T. G. Park, *Nano Today*, 2009, **4**, 429; e) K. Kabiri, H. Omidian, M. J. Zohurrian-Mehr and S. Doroudiani, *Polym. Composite.*, 2011, **32**, 277; f) I. C. Kwon, Y. H. Bae and S. W. Kim, *Nature*, 1991, **354**, 291; g) K. Kataoka, H. Miyazaki, M. Bunya, T. Okano and Y. Sakurai, *J. Am. Chem. Soc.*, 1998, **120**, 12694; h) Z. Wu, X. Zhang, H. Guo, C. Li and D. Yu, *J. Mater. Chem.*, 2012, **22**, 22788; i) A. Wang, Y. Cui, J. Li and J. C. M. van Hest, *Adv. Func. Mat.*, 2012, **22**, 2673; j) P. Zou, J. Suo, L. Nie and S. Feng, *J. Mater. Chem., 2012*, **22**, 6316; k) Y. Takemoto, H. Ajiro, T.-A. Asoh and M. Akashi, *Chem. Mater.*, 2010, **22**, 2923.

8 G. H. Pollack in *Cells, gels and the engines of life: A new, unifying approach to cell function*, *Ebner & Sons*, 2001.
9 L. Zhang, X. Chen, P. Xue, H. H. Y. Sun, I. D. Williams, K. B. Sharpless and V. V. Fokin, *J. Am. Chem. Soc.*, 2005, 127, 15998.
10 J. E. Eldrige and J. D. Ferry, *J. Phys. Chem.*, 1954, **58**, 992.
11 P. Gao, C. Zhan, L. Liu, Y. Zhou and M. Liu, *Chem. Commun.*, 2004, **10**, 1174.
12 D. T. S. Rijkers, G. W. van Esse, R. Merkx, A. J. Brouwer, H. J. F. Jacobs, R. J. Pieters and R. M. J. Liskamp, *Chem. Commun.* 2005, **36**, 4581.
13 E. D. Goddard-Borger and R. V. Stick, *Org. Lett.*, 2007, **9**, 3797.
14 A. Takahashi, M. Sakai and T. Kato, *Polym. J.*, 1980, **12**, 335.
15 P. Fatás, J. Bachl, S. Oehm, A. I. Jiménez, C. Cativiela and D. D. Díaz, *Chem. Eur. J.*, 2013, **19**, 8861.
16 a) P.-A. Ashford and S. P. Bew, *Chem. Soc. Rev.*, 2012, **41**, 957; b) B. K. Hubbard and C. T. Walsh, *Angew. Chem. Int. Ed.*, 2003, **42**, 730; c) A. J. Zhang and K. Burgess, *Chem. Int. Ed.*, 1999, **38**, 634.
17 a) A. Gutowska, Y. H. Bae, J. Feijen and S. W. Kim, *J. Control. Rel.*, 1992, **22**, 95; b) A. Gutowska, J. S. Bark, I. C. Kwon, Y. H. Bae and Y. Cha S. W. Kim, *J. Control. Rel.*, 1997, **48**, 141; d) B. Jeong, Y. H. Bae and S. W. Kim, *J. Control. Rel.*, 2000, **63**, 155.
18 D. J. Overstreet, R. Huynh, K. Jarbo, R. Y. McLemore and B. L. Vernon, *J. Biomed. Mat. Res.*, 2013, **101**, 1437.
19 L. O. White, R. Edwards, H. A. Holf, A. M. Loverling, R. G. Finch and D. S. Reeves, J. Antimicrob. Chemother., 1998, **22**, 739.